END
DATE
FILMED
4 80
DTIC

1.0 ||||

2.8 **2.5**

3.2 **2.2**

3.6

4.0 **2.0**

1.1

1.8

1.25 **1.4** **1.6**

MICROCOPY RESOLUTION TEST CHART
NATIONAL BUREAU OF STANDARDS 1963 A

SECURITY CLASSIFICATION OF THIS PAGE (When Data Entered)

REPORT DOCUMENTATION PAGE		READ INSTRUCTIONS BEFORE COMPLETING FORM
1. REPORT NUMBER	2. GOVT ACCESSION NO.	3. RECIPIENT'S CATALOG NUMBER
4. TITLE (and Subtitle) SHOCK WAVE THERMOMECHANICAL PROCESSING OF AIRCRAFT GAS TURBINE DISK ALLOYS		5. TYPE OF REPORT & PERIOD COVERED Final ~~1 July 1978 to 1 July 1979~~
		6. PERFORMING ORG. REPORT NUMBER FR-11992
7. AUTHOR(s) John M. Robertson, James W. Simon Thomas D. Tillman		8. CONTRACT OR GRANT NUMBER(s) N00019-78-C-0270
9. PERFORMING ORGANIZATION NAME AND ADDRESS United Technologies Corporation Pratt & Whitney Aircraft Group Government Products Division Box 2691, West Palm Beach, FL 33402		10. PROGRAM ELEMENT, PROJECT, TASK AREA & WORK UNIT NUMBERS
11. CONTROLLING OFFICE NAME AND ADDRESS Department of the Navy Naval Air Systems Command Attn: AIR-5163 Washington, DC 20361		12. REPORT DATE August 1979
		13. NUMBER OF PAGES ~~51~~ 54
14. MONITORING AGENCY NAME & ADDRESS(if different from Controlling Office)		15. SECURITY CLASS. (of this report) Unclassified
		15a. DECLASSIFICATION/DOWNGRADING SCHEDULE

16. DISTRIBUTION STATEMENT (of this Report)

Approved for Public Release — Distribution Unlimited.

17. DISTRIBUTION STATEMENT (of the abstract entered in Block 20, if different from Report)

DTIC
ELECTE
MAR 20 1980
B

18. SUPPLEMENTARY NOTES

19. KEY WORDS (Continue on reverse side if necessary and identify by block number)

Shock Wave Processing, Thermomechanical Processing, Turbine Disks, IN-100

20. ABSTRACT (Continue on reverse side if necessary and identify by block number)

This program was conducted to assess the effects of shock wave thermomechanical processing on nickel-base (Ni) gas turbine disks. In particular, the peak pressure limit on shaped subscale turbine disks was determined based on allowable permanent deformation and fracture. Using maximum pressure and selected shock/heat-treat schedules, the effect on mechanical properties was determined with results indicating an enhancement of strength, particularly the yield strength, with only a slight decrease in ductility. In general, low-cycle fatigue (LCF) life was not

DD FORM 1473 EDITION OF 1 NOV 65 IS OBSOLETE
1 JAN 73

S N 0102-LF-014-6601

UNCLASSIFIED
SECURITY CLASSIFICATION OF THIS PAGE (When Data Entered)

392887

significantly affected, however, two samples tested showed a 3X improvement in life. In addition, two shock/heat-treat schedules were found to be extremely beneficial and will be investigated further.

FOREWORD

This report was prepared by Materials and Mechanics Technology Laboratory of the Government Products Division of Pratt & Whitney Aircraft, on U.S. Naval Air Systems Command Contract No. N00019-78-C-0270. Mr. Irving Machlin served as Program Technical Consultant.

The authors are indebted to the Naval Air Systems Command for the opportunity to conduct this investigation and to Mr. Irving Machlin for encouragement and guidance. The authors also acknowledge the help of Dr. J. D. Mote at Denver Research Institute.

This report presents the results of research conducted during the period from 1 July 1978 through 1 July 1979. A continuation of this program on shock wave thermomechanical processing of IN-100 is currently being investigated under Naval Air Development Center Contract No. N62269-79-C-021.

CONTENTS

ILLUSTRATIONS

ILLUSTRATIONS (Continued)

TABLES

SECTION I

INTRODUCTION

Advancements in gas turbine engine technology are largely dependent on extending mechanical property levels of superalloy materials beyond their current temperature limits. The search for more efficient alloys continues, yet new materials have not affected the desired improvements. Material processing developments are also required to supplement alloy development.

Shock wave thermomechanical processing (TMP) has been shown as a viable processing technology and an alternative to conventional deformation processing of cold rolling and/or forging and heat treatment. This technology provides wrought materials with several inherent advantages relative to their rolled/forged counterparts:

1. Near-net shape processing

2. Capability of cold working parts of irregular shape

3. Little or no texturing

4. Fine dislocation substructures promote microstructures with fine precipitate distributions

5. Minimum fracture of carbide particles

6. High vacancy concentration enhances diffusion and improves precipitation response.

Such features are clearly advantageous in the processing of advanced turbine disks. These disks are of irregular shape and can be cold worked only by shock wave TMP with little shape change. Both strength and fatigue properties are enhanced with a specific improvement being made in low cycle fatigue (LCF), the first order property.

This program is sponsored by Naval Air Systems Command (NASC) under Contract N00019-78-C-0270. Its purpose has been to assess TMP parameters, i.e., method of shock loading, heat treatment schedule, shocked part geometry and multiple shocking on the properties of IN-100 (PWA 1074) subscale turbine disks. The major concern of this project has been to demonstrate an improvement in the LCF thermal life of IN-100 turbine disk materials through shock wave TMP. The approach has entailed processing subscale turbine disks (sonic and near-net shape) and flat plates from forged IN-100 powder extrusions, and subsequently shock loading them under various shock/heat treatment schedules via the flyer plate and direct contact methods. A standard unshocked specimen was maintained with each heat treatment as a control. Tensile and LCF properties were evaluated for each processing mode. In addition, transmission electron microscopy (TEM) was used to compare dislocation density levels of IN-100 unshocked materials with both the direct contact and flyer plate shocked materials.

This final technical report includes the results of a 1-year program conducted from 1 July 1978 to 1 July 1979. A continuation of this program has been initiated at P&WA which is designed to optimize the tensile, creep, and LCF properties of shocked IN-100 turbine disk materials. This program will be 15 months in duration.

1

SECTION II

TECHNICAL BACKGROUND

Since 1961, shock wave TMP has been used commercially as a hardening/strengthening process. Every major railroad in this country has adopted this process to harden austenitic manganese steel for trackwork with additional applications, including jaw crushers, swing hammer mills, ore-handling equipment, tread links for power shovels, and cutter teeth for coal-mining machines. In the past, shock wave TMP benefits have been suppressed because of the observed and accepted brittle response in ferritic steels. Presently, usage of shock wave TMP material is increasing as investigators demonstrate better ductility, toughness, LCF and creep properties.

The two basic methods that have been used in shock wave TMP studies conducted over the past 20 years are flyer plate and direct contact shocking. The direct contact technique has been used in the commercial shock wave applications discussed previously. Both methods have proven to be capable of hardening irregularly shaped materials, although higher pressures coupled with better directional control of the shock wave are attained with the flyer plate approach.

Flyer plate shocking has been the most popular method in shock wave TMP studies of nickel-base superalloys. The effects of shock wave TMP have been investigated with alloys AF2-1DA, Inconel 718 and Udimet 700. The respective shocked/unshocked alloy pairs were evaluated in the same heat treated state. Each of these materials demonstrates a general increase in both their room temperature yield and ultimate tensile strengths in the shocked vs unshocked condition, although a significant reduction in ductility was also observed. The shocked material in each case exhibited longer *LCF and stress rupture life up to* 1200°F (649°C). The AF2-1DA alloy demonstrated longer LCF life in the shocked state to 1400°F (760°C). In addition, tensile ductility improvements were found in shocked Inconel 718 and Udimet 700 to 1200°F (649°C) and in the AF2-1DA alloy to 1400°F (760°C).

The strength improvements observed in the shock-loaded alloys tested have been explained as resulting from a very fine dislocation substructure pinned by γ', γ'' or carbide precipitates. These fine dislocation substructures are effective in reducing the mean free path for dislocation movement.

The importance of a predeformation treatment has been emphasized in each of these materials. Aging prior to shocking results in greater precipitate/dislocation interaction which contributes to the effectiveness of precipitates to pin dislocations, thus improving strength.

Final postdeformation aging treatments in these materials causes a homogeneous precipitation of $M_{23}C_6$ particles on dislocations which further contributes to improved strength. A final age in the Inconel 718 alloy has been reported to promote a more heterogeneous nucleation of γ' precipitates on dislocations which should also hinder further dislocation motion, although some coarsening of existing γ' particles may also occur.

High dislocation density and twinning have been shown characteristic of explosively-strengthened materials. Each of these factors may contribute to the total strengthening effect in shocked nickel-base superalloys. It has been established that the flow stress of deformed materials increases linearly with increasing dislocation density. In a heavily worked structure, high dislocation density regions develop into tangled networks and form a cellular substructure with high-density dislocation tangles making up the cell walls. This formation in itself contributes to further strengthening. Friedel has explained that the passage of a dislocation

through a twinned crystal requires additional dislocations to be generated.* This production of dislocations requires energy and necessarily increases the applied shear stress required to generate and move dislocations.

In contrast with cold rolling, the shock wave TMP of metals has been shown to achieve higher hardness at a given level of true strain and greater toughness at a given strength level. The former has been clearly demonstrated by Appleton and Waddington for copper, while Peitteiger has achieved better toughness with stainless, nickel, manganese and carbon steels, Inconel and other materials in the shocked vs cold-rolled hardened state.* In addition, Orava observed with Udimet 700 an order of magnitude less in the spacing between active {111} slip planes in the shock hardened than the 52% cold reduced condition.* The result is evidence that slip is on a finer scale and necessarily more difficult in shock loaded than cold-rolled Udimet 700.

---

*A list of references appears at the end of this report.

3

SECTION III

EXPERIMENTAL PROCEDURE

This program was to establish the effects and feasibility of shock-loading turbine disks made of the nickel-base alloy, IN-100 (MOD). This alloy was selected since it is the Bill of Material (B/M) for turbine disks in the F100* engine. Current parts are limited in LCF and the program is aimed at achieving improvements in this area with an attendant increase in strength.

IN-100 (MOD) was purchased as a wrought powder metal product conforming to PWA 1056 specifications. The nominal composition is shown below:

Ni	Cr	Co	C	Ti	Al	Mo	V	Zr	B	
bal	12.4	18.5	0.07	4.3	5.0	3.2	0.8	0.06	0.02	(wt %)

It was required that peak pressures used on flat plates for the determination of mechanical properties be established for shaped parts so that the data obtained would be more meaningful with regard to engine hardware. To this end, two subscale turbine disk shapes (Figures 1-4) were selected for peak pressure determination. They are representative of both sonic and near-net shaped (NNS) sections that would be encountered on a production basis. The subscale disks were GATORIZED® from preform sizes of 5.1 (13.0) by 0.372 in. (0.945 cm) (NNS) and 5.0 (12.7) by 0.887 in. (2.254 cm) (sonic) in P&WA's vacuum isothermal forging press at a metalworking temperature of 2050°F (1151°C). In order to achieve full shape definition, the forging flash was machined from appropriate areas of the disks which were then reforged to the final shape. The disks were then grit blasted, to remove any lubricants used in the forging operations, prior to heat treatment.

Material for flat plates was obtained from the same log of IN-100 as the shaped disks. It was to be re-extruded to a smaller diameter for forging preforms and forged to pancakes. This was to ensure that the flat plates were forged an amount equivalent to the subscale disks. During the extrusion process the billet was exposed to a temperature above that specified and was destroyed. In order to replace the material that was lost, without major penalties in scheduling, the center sections of production F100 2nd-stage turbine spacers were used. These plates were nearly identical to those originally planned. They differed only in that the center of the plates contained a small dimple. They were machined to 6.0 in. (16.2 cm) dia by 0.6 in. (0.162 cm) thickness. A cross section of these plates is shown in Figures 5 and 8.

HEAT TREATMENT

Five different heat treatments were selected for the shocking of flat plates for mechanical test specimens. In order to directly assess the effects of shockwave deformation (SWD), one plate of each heat treatment was processed thermally without shocking. This yielded property differences due to heat treatment in addition to variations due to shocking parameters. The heat treat schedule is shown in Table 1.

All of the shaped parts used for peak pressure determination were given the overage heat treatment designated "B" in an effort to minimize fracture at shocking by having the material in a lower strength, higher ductility condition.

Indications from the literature* are that any heat treatment above 1400°F (760°C) causes sufficient thermal recovery to negate beneficial effects due to shocking. For this reason only the low temperature γ' and final ages were applied after shocking. Heat treatment A eliminates the stress relief cycle (SR) and allows for γ' precipitation of the solutioned and shocked structure.

*A list of references appears at the end of this report.
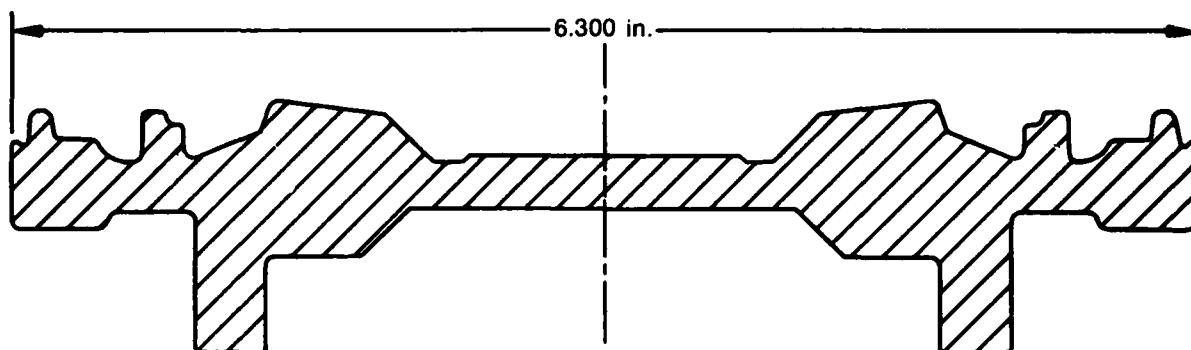
Figure 1. Cross Section of Subscale F100B 1st-Stage Turbine Disk, Sonic Shape
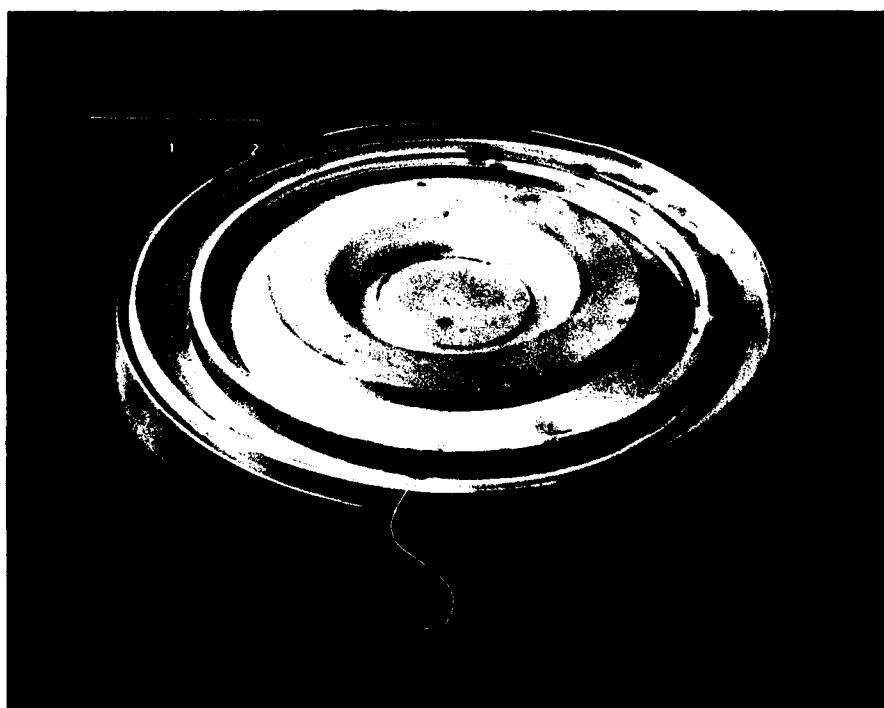
Figure 2. Subscale F100B 1st-Stage Turbine Disk, Sonic Shape

—5.812 in.—
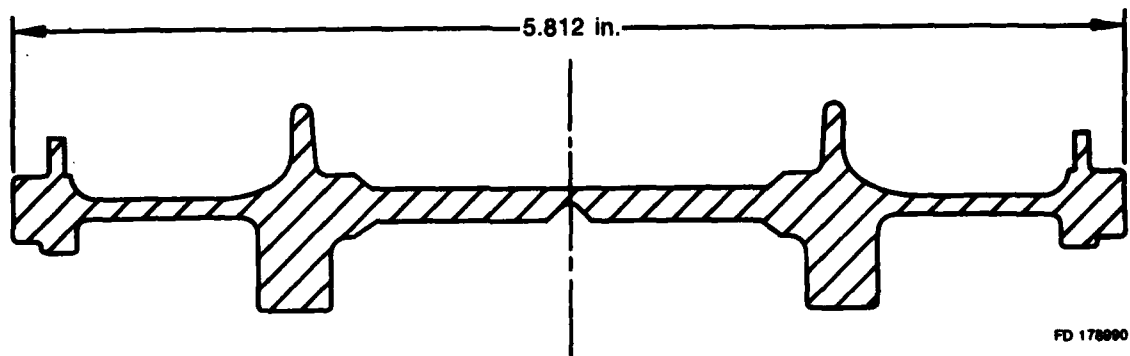
FD 178990

Figure 3. Cross Section of Subscale F100B 3rd-Stage Turbine Disk, Near-Net Shape

FE 172695
FD 178991

Figure 4. Subscale F100B 3rd-Stage Turbine Disk, Near-Net Shape

6

0.6 in.

6.0 in.
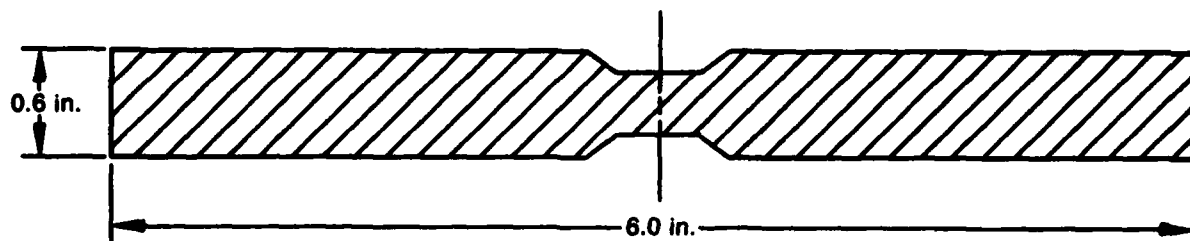
FD 178882

Figure 5. Cross Section of Flat Plate for Mechanical Testing

Mag: ½X
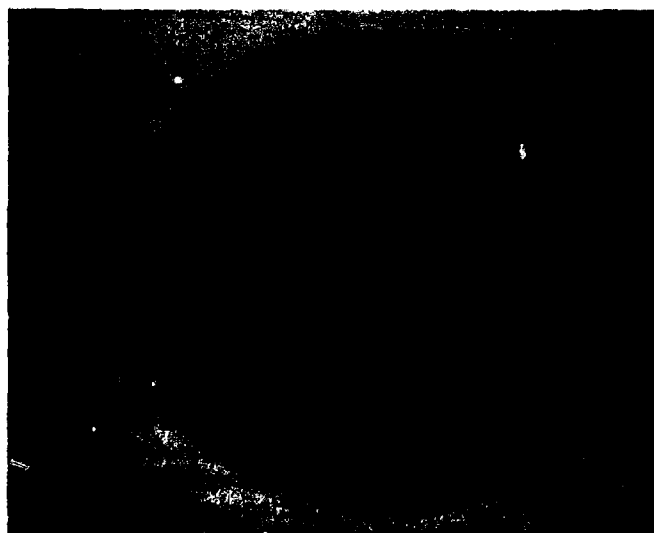
FAL 54865

Top View

FD 178883

Figure 6. Macrograph of Flat Plate for Testing Program

7

TABLE 1. HEAT TREATMENT SCHEDULE FOR FLAT PLATES OF IN-100ϕ

Plate No.	Sol.	Stress Relief	Shock	γ'	Final
A1, A2	2065°F, 2h, OQ	—	150 kbars**	1200°F, 24h, AC	1400°F, 4h, AC
A3	2065°F, 2h, OQ	—	2g/in.²†	1200°F, 24h, AC	1400°F, 4h, AC
A4	2065°F, 2h, OQ	—	None	1200°F, 24h, AC	1400°F, 4h, AC
B1, B2	2065°F, 2h, OQ	1900°F, 3h, AC	150 kbars**	1200°F, 24h, AC	1400°F, 4h, AC
B3	2065°F, 2h, OQ	1900°F, 3h, AC	2g/in.²†	1200°F, 24h, AC	1400°F, 4h, AC
B4	2065°F, 2h, OQ	1900°F, 3h, AC	None	1200°F, 24h, AC	1400°F, 4h, AC
C1, C2	2065°F, 2h, OQ	1600°F, 40 min, AC 1800°F, 45 min, AC	150 kbars**	1200°F, 24h, AC	1400°F, 4h, AC
C3	2065°F, 2h, OQ	1600°F, 40 min, AC 1800°F, 45 min, AC	2g/in²†	1200°F, 24h, AC	1400°F, 4h, AC
C4*	2065°F, 2h, OQ	1600°F, 40 min, AC 1800°F, 45 min, AC	None	1200°F, 24h, AC	1400°F, 4h, AC
D1, D2	2065°F, 2h, OQ	1600°F, 40 min, AC 1800°F, 45 min, AC	150 kbars**	1200°F, 8h, AC	1400°F, 4h, AC
D3	2065°F, 2h, OQ	1600°F, 40 min, AC 1800°F, 45 min, AC	2g/in.²†	1200°F, 8h, AC	1400°F, 4h, AC
D4	2065°F, 2h, OQ	1600°F, 40 min, AC 1800°F, 45 min, AC	None	1200°F, 8h, AC	1400°F, 4h, AC
E1, E2	2065°F, 2h, OQ	1600°F, 40 min, AC 1800°F, 45 min, AC	150 kbars**	1200°F, 8h, AC	1400°F, 2h, AC
E3	2065°F, 2h, OQ	1600°F, 40 min, AC 1800°F, 45 min, AC	2g/in.²†	1200°F, 8h, AC	1400°F, 2h, AC
E4	2065°F, 2h, OQ	1600°F, 40 min, AC 1800°F, 45 min, AC	None	1200°F, 8h, AC	1400°F, 2h, AC

*Standard PWA 1074 heat treatment
**Flyer plate shocked
†Direct contact shocked
ϕ2065°F = 1129°C, 1900°F = 1138°C, 1800°F = 982°C, 1600°F = 871°C, 1400°F = 760°F, 1200°F = 649°C

However, heat treatment B provides an overaged structure to hopefully pin dislocations during shocking. The P&WA standard heat treatment for IN-100 is represented by C and was used for that reason. D and E are variations of the standard treatment with shorter γ' and final aging cycles. The shorter times were chosen because shocking is known to create defects which could enhance diffusion and cause overaging if standard times were used.

MECHANICAL TESTING PROCEDURE

Tensile tests were performed at elevated temperatures simulating conditions observed in turbine disks. Testing was conducted at 1000°F (538°C) and 1200°F (701°C) in air at a strain rate of 0.005 in./in./min (cross head speed = 0.15 in./min (0.38 cm/min)). Elevated temperatures were controlled to ±5°F (2.7°C) with chromel-alumel thermocouples in contact with the specimen at both ends of the gage section. The specimen configuration used was a round tensile bar machined from the flat plates and is shown in Figure 7.

Low-cycle fatigue testing was done in air at elevated temperatures of 1000°F (538°C) and 1200°F (649°C) controlled by means of a chromel-alumel thermocouple in contact with the specimen gage section. A strain range of 0 to 1.0% was used cycled about the mean strain of 0.5% at 10 cycles per min (0.166 Hz). The specimen is shown in Figure 8. LCF specimens were taken tangentially from shocked plates since this is where the primary stresses are observed in actual parts.

In order to optimize the evaluation of tensile and LCF results a test matrix, shown in Table 2, was devised to provide a data cross section suitable for statistical analysis. It was assumed that no difference existed between plates 1 and 2 shocked by the flyer plate method, and 3 and 4 shocked by direct contact. Ten additional tests labeled repeats are included to determine any variation from plate to plate within a given process and heat treatment.

8

Figure 7. Standard Round Bar Tensile Specimen

Center Holes Permitted
Both Ends

45° Cham
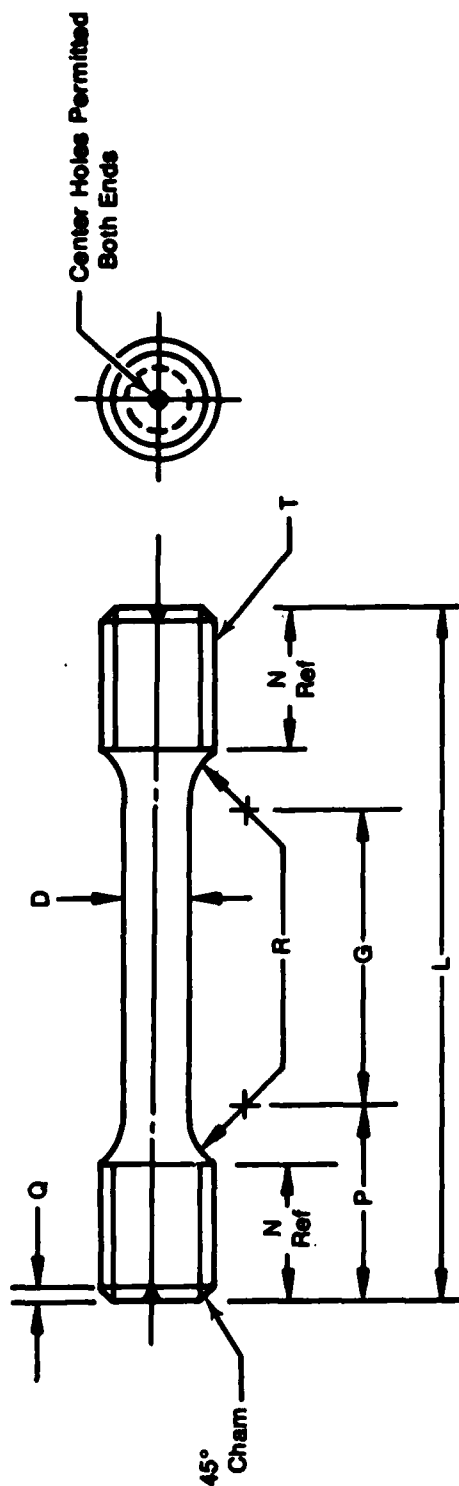
Notes

1. All Dimensions in Inches
2. Tolerances ± 0.010 Unless Noted
3. All Dia To Be Conc to Within 0.001 FIR
4. Reduced Section To Be 16 ± 3μ in. AA Grind Finish Using 320 Grit Wheel
5. Dia of Reduced Section To Be Slightly Smaller at Center than at Ends (Approx 0.0015), but Not to Exceed 1% of Larger Dia
6. Identification Markings Permitted Only on Specimen Ends

Spec No.	D	G	L	N	P	Q	R	T
±0.001								
6"	0.252	1.062	2.750	0.625	0.844	0.065	0.250	0.500 - 13 UNJC-3A

FD 178884

Figure 8. *Strain Control Low Cycle Fatigue Specimen*

All Dimensions in Inches

Notes

① Tangent Points of 1.750 Rad and 0.075 Rad Must Be Blended Smoothly, No Undercuts or Ridges Permitted

② Center of 1.750 Rad Must Be Located Within 0.004 of Transverse ₵ of Gage

③ All Diameters To Be Concentric Within 0.002 FIR

④ Gage Section To Be 8 ± 3 Microinches AA Grind Finish, Including Inboard Collar Faces

⑤ Work to Dimensions, Do Not Scale

⑥ Identification Markings Permitted Only on Ends of Specimen

⑦ Locate ₵ Within 0.010 of Overall Specimen Length Refer to View 'A' for All Other References to this ₵

TABLE 2. TENSILE TESTING MATRIX

| | Heat Treatments | | | | | | | | | |
| | A | | B | | C | | D | | E | |
	1000°F (538°C)	1300°F (704°C)	1000°F (538°C)	1300°F (704°C)	1000°F (538°C)	1300°F (704°C)	1000°F (538°C)	1300°F (704°C)	1000°F (538°C)	1300°F (704°C)
Flyer Plate 1	T			T	T		T			T t
Flyer Plate 2		T	T		T t			T	T	
Direct Contact 3	T	T	T	T	T	T	T t	T	T	T
Control 4	T	T t	T	T	T	T	T	T	T	T

| | LCF Testing Matrix | | | | | | | | | |
| | A | | B | | C | | D | | E | |
	1000°F (538°C)	1200°F (649°C)	1000°F (538°C)	1200°F (649°C)	1000°F (538°C)	1200°F (649°C)	1000°F (538°C)	1200°F (649°C)	1000°F (538°C)	1200°F (649°C)
Flyer Plate 1	F			F	F		F f			F
Flyer Plate 2		F f	F		F			F	F	
Direct Contact 3	F	F	F	F f	F f	F	F	F	F	F
Control 4	F	F	F f	F	F	F	F	F	F	F f

T = tensile test t = tensile repeat
F = fatigue test f = fatigue repeat

METALLOGRAPHIC PROCEDURES

Standard procedures were used in the preparation of IN-100 surfaces for optical microscopy. Grinding through 600 grit silicon carbide paper was followed by mechanical polishing with 6μ and 1μ diamond paste. Samples were etched with glyceregia or Kalling's.

Preparation of thin foils of IN-100 for transmission electron microscopy was performed on samples from heat treatments A, B, and C of all three processing methods, i.e., flyer plate, direct contact shocking and control processes. Initial slices from processed plates of approximately 50 mils thickness were ground on 320 grit silicon carbide paper to 15 mils by alternating sides every 2 to 3 mils. Subsequently, specimens were ground to a 5 mils thickness on 600 grit paper in a similar fashion. Specimens 0.12 in. (3mm) in dia were then punched from the desired locations of the 5 mil sample for subsequent thinning operations.

Preparation of electron transparent regions was accomplished with a Fischione Model 110 electropolishing unit used in conjunction with a Model 120 power controller. The electrolyte, 13% H_2SO_4 in methanol, was held between 5 and 14°F (−15 and −10°C) and minimum detectable jet flows were utilized during polishing. Current settings varied with each specimen in the 40 to 60 mA range at 20V.

SHOCK LOADING PROCEDURES

All shock work and calculations of the necessary parameters involved were conducted at Denver Research Institute under P&WA direction.

It was decided that two shocking methods be investigated during this program: the flyer plate and direct contact methods. Each method has certain advantages. For example, the flyer plate method is used most often in experimental work since it allows independent variation of peak pressure, pulse duration, and rarefaction rate. Direct contact shocking is amenable to processing local areas such as the rim or bore sections of a turbine disk.

Figures 9 and 10 show schematic drawings of shock waves propagating into the sample by the flyer plate and direct contact methods. When shocking by flyer plates, the peak pressure (Pm) exists for a short period of time which is referred to as pulse duration, f_p. Immediately thereafter the peak pressure decays with time to zero. The distance the maximum pressure travels into the target, X_p, is given by

$$X_p = t_p \cdot U_s$$

where U_s is the shock wave velocity. When shocking using the direct contact method, any reference to pulse duration is meaningless since the peak pressure attenuates immediately. The movement of dislocations through the plate occurs at a threshold pressure below which dislocations are immobile. Therefore, not only is peak pressure an important parameter, but also pulse duration as well.

The determination of peak pressures for mechanical testing specimens was done on shaped parts to establish the feasibility of the process to real world engine applications. A peak pressure of 100 kbar was chosen as a starting point on both the near-net and sonic-shaped disks. It was decided that the peak pressure for test specimens would be the maximum pressure tolerable with no fracture or undesirable permanent deformation in shaped parts. Iterations about the starting pressure were done to establish that peak pressure.
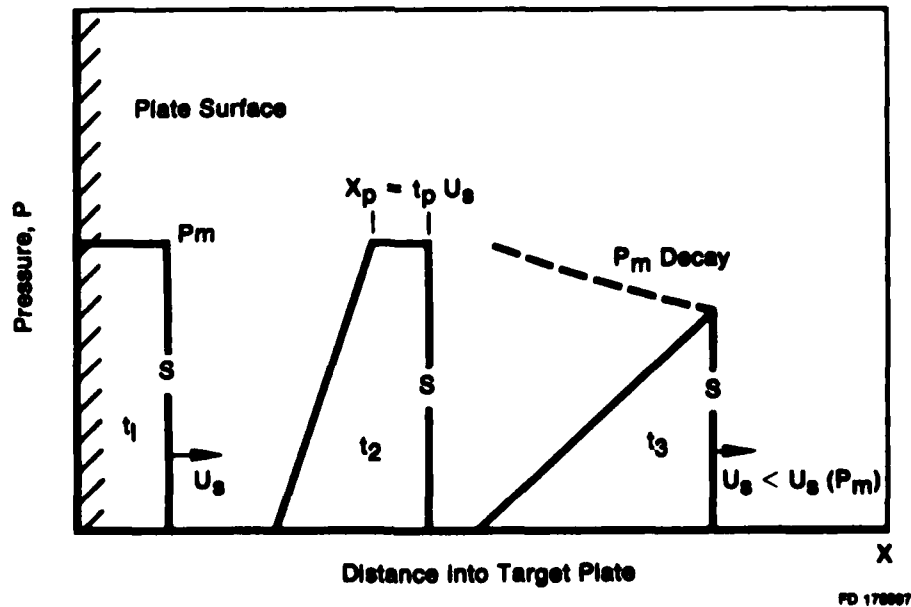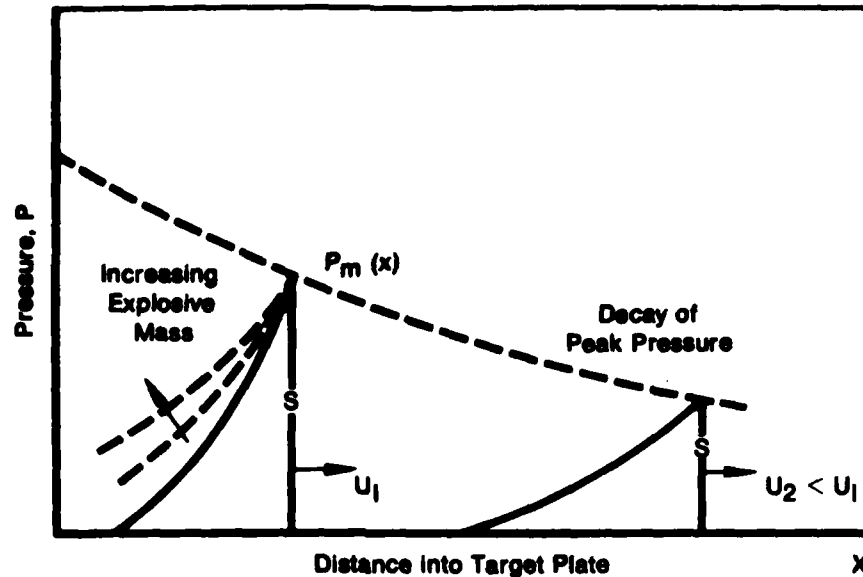

Figure 9. Propagation and Attenuation of a Plastic Shock Pulse Due to Plate Impact

Figure 10. Shock Pulse Profiles Due to Contact Explosive

Figure 11 shows a schematic diagram of the shock wave apparatus. The target (shaped disk or flat plate) was potted in a spall ring with a low melting point metal or alloy, in this case lead (Pb). Specimens were lubricated to aid the removal from the Pb. The spall ring was made of mild steel and was 1.5 in. thick. The supporting anvil and flyer plate were mild steel also. A simulated plane wave generator was used to accelerate the flyer plate, which consisted of approximately 20 detonator cord sections of the same length set in a pattern of concentric circles which would allow simultaneous detonation of the Detasheet C explosives at these locations. Direct contact explosives were ignited in a similar manner. The entire assembly was supported over a cardboard barrel filled with water such that the specimens were quenched immediately after shocking to prevent any thermally induced effects.

As indicated previously, 3 parameters, peak shock pressure, shock pulse duration and rarefaction rate, can be varied independently. For the purposes of this program, any effects due to rarefaction rate will be ignored. In addition, pulse duration will be held relatively constant while the peak pressure is varied. A method for calculating the amount of explosives required at a given shock pressure will be explained. First, a shock pressure is assumed which is applied to the known Rankine-Hugoniot curves of peak pressure vs particle velocity (U_p) can then be obtained for the various materials to find V_p, the velocity of the flyer (driver) plate in the equation below:

$$V_p = U_p^T + U_p^D.$$

13
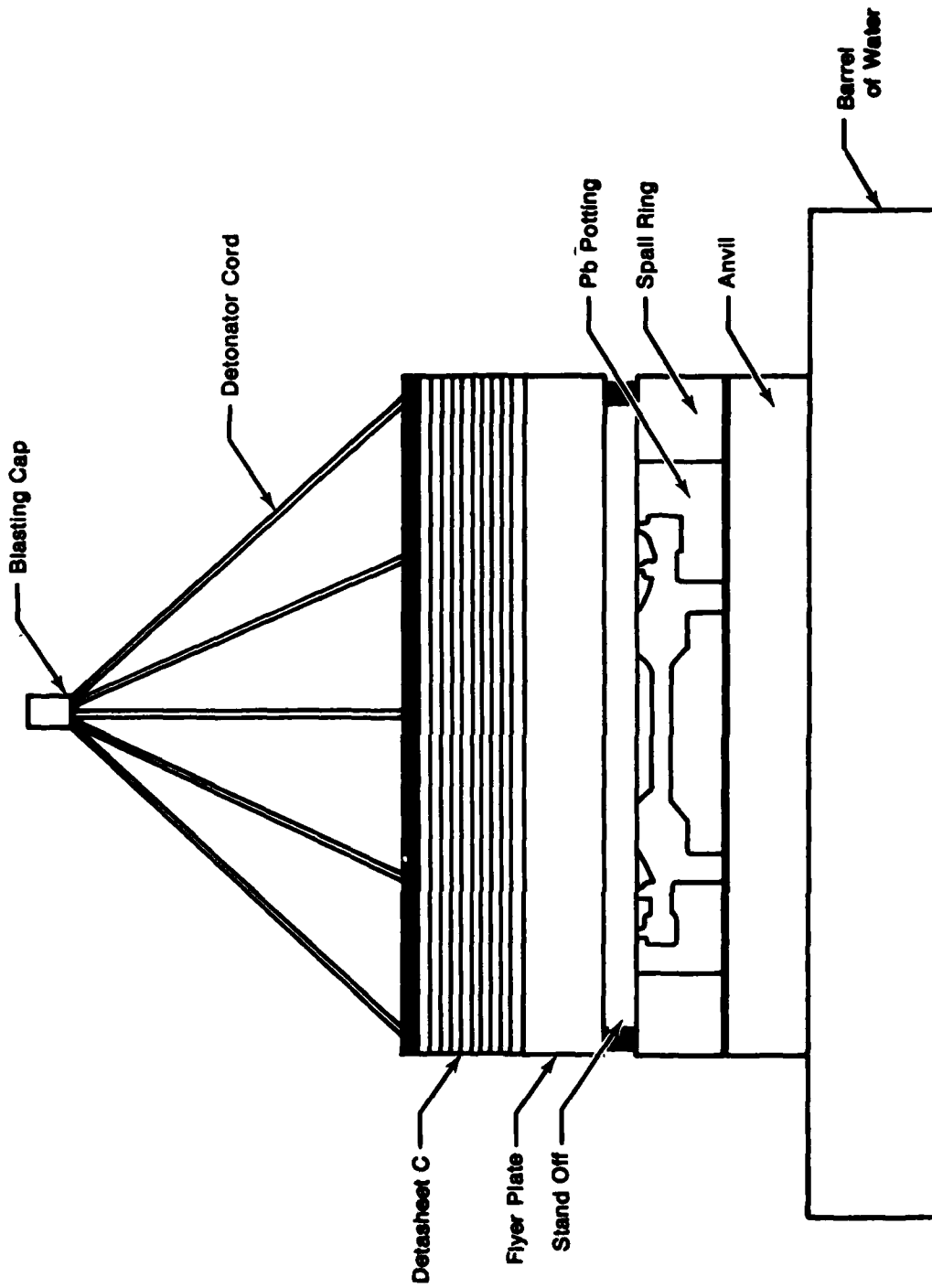
Figure 11. Shock Wave Apparatus, Simulated Plane Wave Generator

14

This equation states that the velocity of the flyer plate is the sum of the particle velocities of the driver plates, $U_p{}^D$, and target materials, $U_p{}^T$. It is often difficult to obtain information regarding complex alloys. An approximation of the Rankine-Hugoniot curve for IN-100 can be made with the curves of the various elemental constituents within the alloy by the law of mixtures for the atomic percentages present. The pressure particle velocity curve for 304 s/s is reasonably representative of IN-100 (Figure 12). Once the velocity of the driver plate at a given pressure is obtained, it is necessary to calculate the amount of explosives required for that velocity. The equation developed for that purpose by Gurney in 1943 for conditions of plane wave shock generation is:

$$V_p = \sqrt{2\,E}\ [\ 3/(\ 1 = 5(M/C) + 4\ (M/C)^2)\ ]^{\prime\prime}.$$

where V_p is the driver plate velocity under steady-state conditions, M is the driver plate mass, C is the mass of explosive, E is the "Gurney energy" per unit mass of explosive, and $\sqrt{2\,E}$ is termed the "Gurney characteristic velocity" of the explosive. Finally, C, the mass of explosive, can be calculated by assuming, or measuring a drive plate mass.

Of prime importance in flyer plate experiments, is stand-off distance, which is that distance which separates the driver plate and target sufficiently to allow the driver plate to achieve terminal velocity on impact. For the purposes of this program an empirical equation was used which relates the thickness of the driver plate and explosive to the stand-off distance. The equation reads:

$$d_s = 0.2\ (d^D + d^E)$$

where d_s is the stand-off distance, d^D is the thickness of the driver plate and d^E is the thickness of the explosive.

The *pulse duration occuring during shock* loading was approximately 8 μsec and can be estimated from the following equation:

$$t_p = d^D\ (1/U_s{}^D + \rho_o{}^D/\rho^D C^D)$$

where t_p is pulse duration, $U_s{}^D$ is the shock velocity of the driver plate, $\rho_o{}^D$ and ρ^D indicate densities ahead and behind the shock front, respectively, and C^D refers to the velocity of sound within the driver plate. The variables required can be obtained from Hugoniot data.
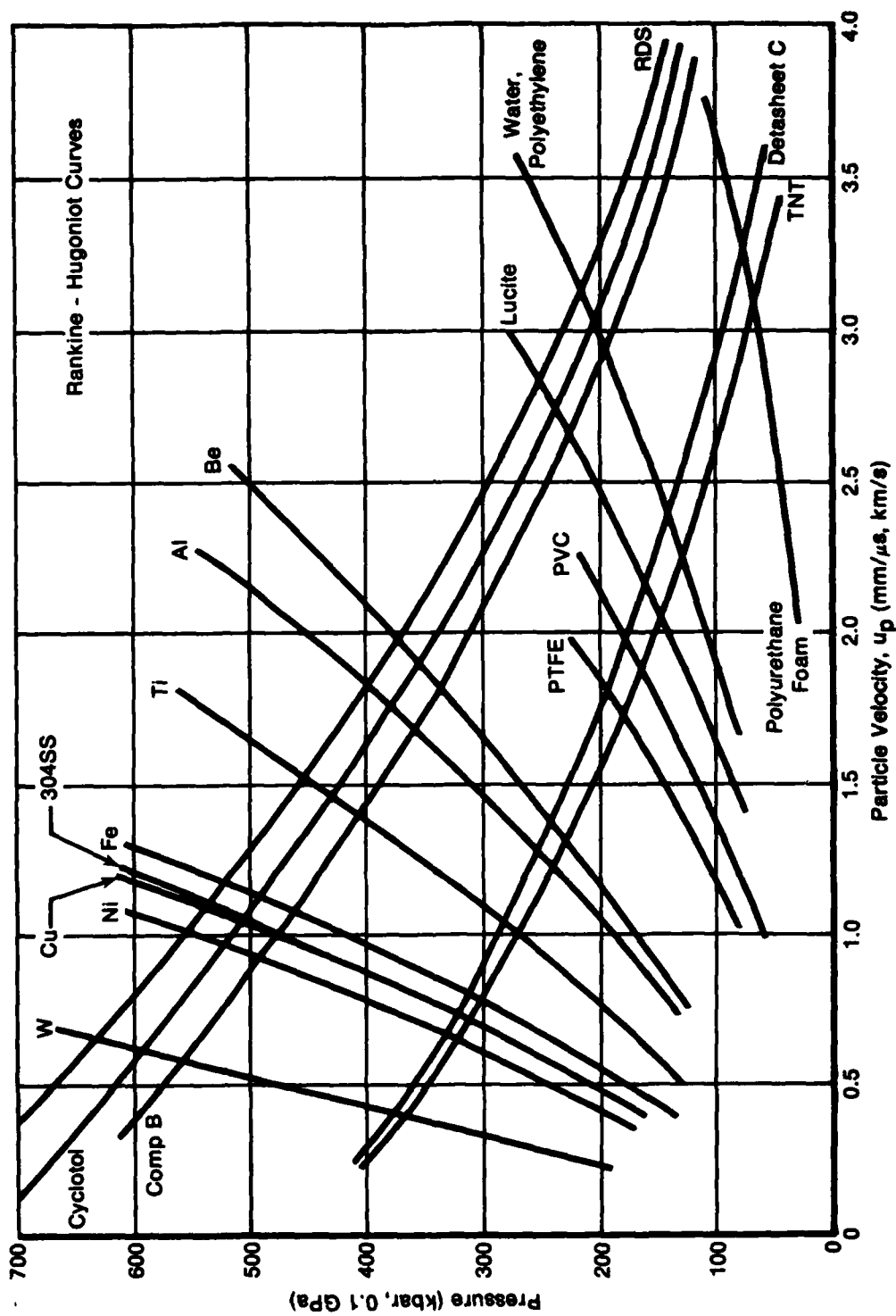
Figure 12. *Shock Waves Induced in Various Metals by Normally-Incident Plane Detonation Waves*

16

SECTION IV

RESULTS

Experiments were conducted to assess the effects of shock wave processing on the properties of IN-100 (MOD) of various heat treatments. The shocking process caused approximately a 10% transient stain, whereas the overall dimensional change was less than 1%.

Figures 13 through 16 are macro photographs of shocked disks. The first shock trial by the flyer plate method on a near-net shaped disk (Figure 13) was done at 100 kbars. The disk did not retain its shape and fractured. Subsequent attempts were conducted at 75 kbars. Figures 14 and 15 showed slight cracking but on the final attempt the disk remained intact (Figure 16).

The sonic shaped disks were able to withstand higher pressures than the near-net shaped disks with the peak pressure being 150 kbars. Disks were intact after shocking at 100 and 125 kbars, but slight cracking was observed at 150 kbars (Figures 17 and 18).

Direct contact work was successful on all but one attempt. Loading at 2g/in.^{2} proved to be too high for near-net shaped disks and the explosive sheared the bore area as shown in Figure 19. 2g/in.^{2} was withstood by sonic disks and was decided on as the pressure for direct contact work. Shock pressure in direct contact loading is given as weight (in grams) per unit area (in inches) vs the kbar pressure calculated in flyer plate work.

TENSILE PROPERTIES OF IN-100 CONTROL SAMPLES

Tensile bars were obtained from flat plates of material conforming to P&WA Specification 1074, which is powder processed forged IN-100. Five different heat treatments were employed in the test program with one plate being heat treated without chocking for control purposes. One of the heat treatments conformed to the standard 1074 heat treatment (C4 in Table 1). The nominal values of the P&WA 1074 material for yield, tensile strength, percent elongation and reduction in area are listed in Table 3 along with the data obtained during the program for unshocked specimens. All of the specimens tested exceeded the mean requirement for yield strength with the exception of the B4 samples which were slightly lower due to the over aged heat treatment. However, they did conform to the 95% lower limit. As far as ductility is concerned, only sample A4 tested at 1300°F (704°C) did not exceed the mean values for ductility, but did fall within the 2σ lower bound. It is interesting to note that while the plot of yield strength vs temperature in the range 1000 to 1300°F (538 to 704°C) is relatively flat, changing only a few ksi in 300°F (167°C), the corresponding curve for ultimate strength drops sharply with temperature, 35 ksi (241.5 MPa) over the same range.

17

Mag: ½X   FAL 54073

Top

Mag: ½X   FAL 54073

Bottom

                                           FD 184252

Figure 13.   Near-Net Shaped Disk Shocked at 100 kbar Pressure

Mag: ½X

FD 184253

Figure 14.   Near-Net Shaped Disk Shocked at 75 kbar With Cracking
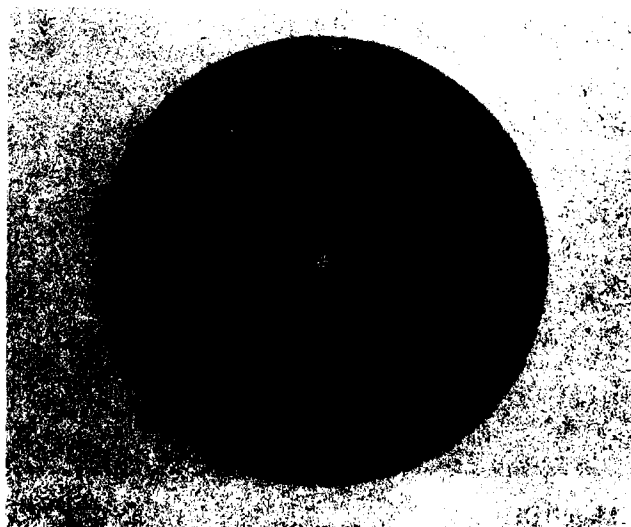
Mag: ½X   FAL 54070

Near-Net Shaped

FD 184254

Figure 15.   Near-Net Shaped Disk Shocked at 75 kbar With Cracking

Mag: ½X   FAL 54071
                    Top

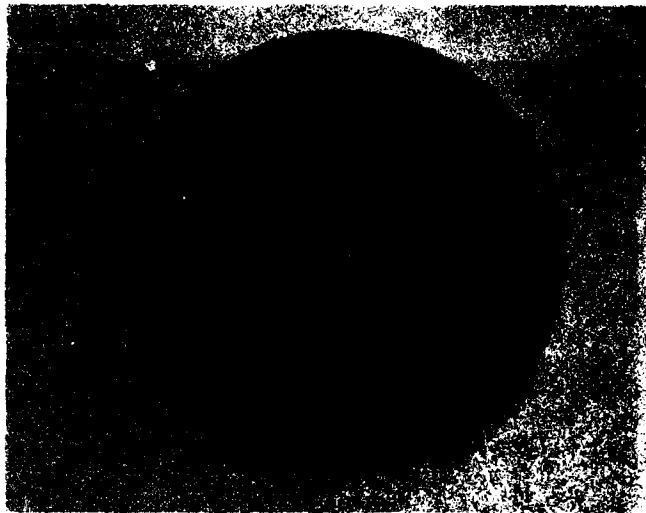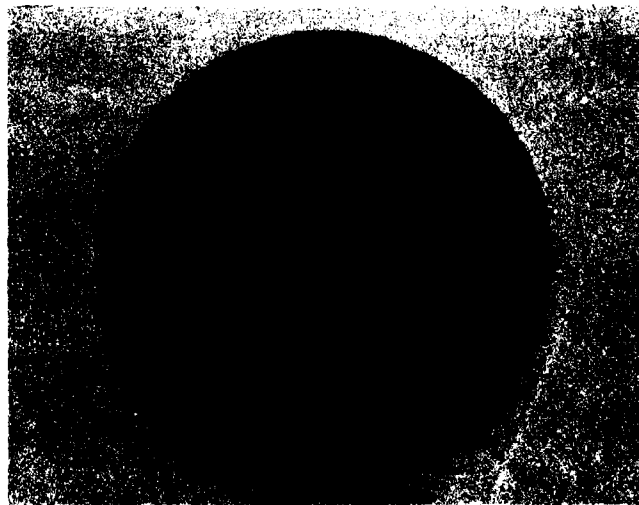Mag: ½X   FAL 54072
                  Bottom
                                  FD 184255

Figure 16.   Near-Net Shaped Disk Successfully Shocked at 75 kbar Pressure

Mag: ½X

FD 184256

Figure 17.   Sonic Shaped Disks Shocked at 150 kbar, With Slight Cracking

Mag: ½X

FD 184257
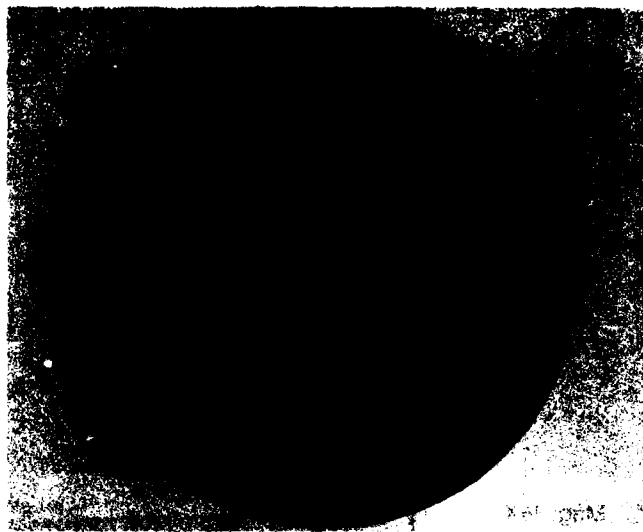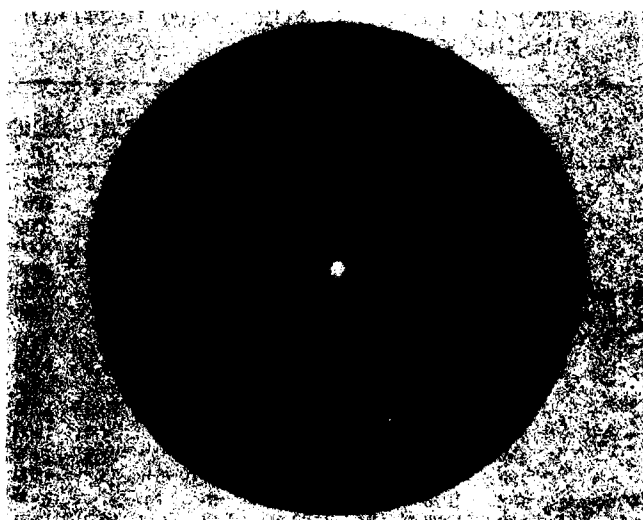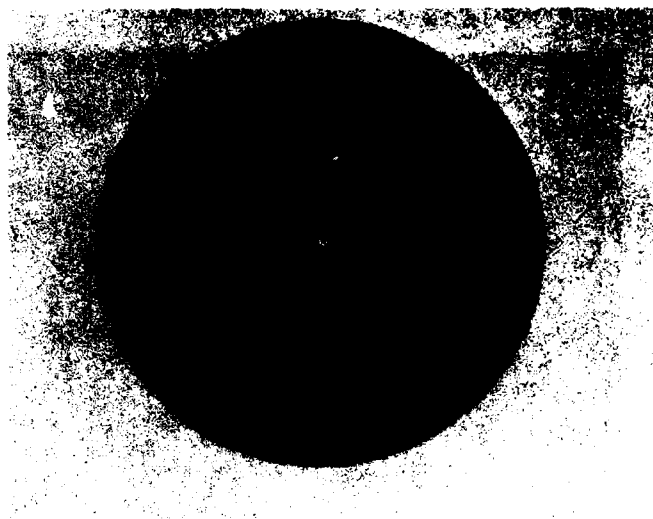
Figure 18.   Sonic Shaped Disks Shocked at 150 kbar With Cracking

21

Mag: ½X

FAL 54052

FD 184258

*Figure 19.   Near-Net Shaped Disk Shocked on One Side With Direct Contact
Explosives at 2G/in? With Sheared Bore Area*

TABLE 3.   TENSILE RESULTS FOR IN-100 CONTROL SAMPLES
(UNSHOCKED)

Plate No.	0.2% Offset Yield Strength (ksi)	(MPa)	Ultimate Strength (ksi)	(MPa)	Elongation (%)	RA (%)	Temperature (°F)	(°C)
A4	167.5	1154.1	228.0	1570.9	22.5	20.2	1000	(538)
B4	157.0	1081.7	215.6	1485.5	28.5	26.6	1000	(538)
C4*	161.4	1112.0	222.5	1533.0	25.0	24.1	1000	(538)
D4	160.9	1108.6	223.0	1536.5	27.0	26.8	1000	(538)
E4	159.7	1100.3	220.4	1518.6	26.5	27.3	1000	(538)
PWA 1074* mean	159	1095.5	217	1495.1	22	20	1000	(538)
95% lower bound	152	1047.3	209	1440.0	16	13	1000	(538)
A4	166.1	1144.4	190.3	1311.2	17.0	19.0	1300	(704)
A4	166.6	1147.9	188.9	1301.5	20.5	21.4	1300	(704)
B4	156.7	1079.7	175.8	1211.3	27.0	30.6	1300	(704)
C4*	159.6	1099.6	182.2	1255.4	21.5	24.4	1300	(704)
D4	159.0	1095.5	181.0	1247.1	19.5	22.4	1300	(704)
E4	159.5	1099.0	179.8	1238.8	21.0	24.1	1300	(704)
PWA 1074* mean	158	1088.6	182	1254.0	18	21	1300	(704)
95% lower bound	150	1033.5	174	1198.9	13	12	1300	(704)

*P&WA standard IN-100 (MOD) heat treatment

TENSILE RESULTS FROM SHOCKED SAMPLES

Results obtained from tensile testing are shown in Table 3. Due to the small number of tests made, it is difficult to make absolute statements concerning property improvements due to heat treat or shock wave processing. General statements regarding data trends will be made, but further testing would be necessary to verify these trends. As expected, it appears that shocking by either method causes an increasing in yield strength. The flyer plate method gives larger improvements but at the expense of lower ultimate strength and ductilities of less than 10% in most cases. In general, the flyer plate process produced the strongest material followed by direct contact. The control samples were the weakest. However, there was one anomaly in this trend. The mean ultimate strength of material tested at 1000°F was highest for direct contact processing, and material shocked by the flyer plate method actually showed a debit in strength when compared to the control samples. At the 1300°F (704°C) test temperature, this behavior did not occur and the processes ranked as before. As mentioned previously there is minimal change in the yield strength of IN-100 over the range 1000 to 1300°F (538 to 704°C). This observation was supported by the testing conducted on shockwave samples. While the strength improved due to shocking, there were no indications that test temperature had any effect on the strengthening mechanisms produced by shocking, within the range studied. Ductilities measured were highest for the control samples. A small decrease of 3 to 4% was observed in direct contact samples, and a significant debit of 8 to 9% occured in flyer plate samples. This decreased ductility was expected in light of the increased strength observed.

Variations in properties due to heat treatment were more difficult to assess. Of the five heat treatments examined, C, D and E are nearly the same and varied only the hold times for the post-shock aging treatment. This was done to determine if the creation of point defects due to shock treatments would affect the diffusion and aging response of this alloy. The tensile results are quite similar and there appears to be no significant difference between them (Table 4). Heat treatment A, which eliminated the preshock stress relief cycle, showed higher strengths but once again, at the expense of ductility. Heat treatment B produced an overaged structure designed to pin dislocations. In this case the strength was lower than all the other heat treatments, but ductility did not suffer.

Results obtained from low cycle fatigue testing are shown in Table 5 and Figures 20 and 21 along with the accepted mean and lower bound for standard PWA 1074 material. The data reported at 1000°F (538°C) were the most promising. Although the majority of the tests made produced results which are scattered about the mean, two tests look very promising. Sample A3, direct contact shocked, failed after 14,670 cycles compared to the mean of 4,550 cycles. In addition, sample C2, flyer plate shocked, failed at 16.030 cycles. Examination of the fracture surface revealed an internal failure as shown in the fractographs in Figure 22. Further investigation of stereo pairs indicates the initiation occurred at a void. Several tests were not performed due to machining defects detected prior to testing; and time did not permit remachining. Specimen E2, which failed on set-up, was examined by scanning electron microscopy (SEM) and these fractographs are shown in Figure 23. The fracture appearance indicates an overload dimple rupture failure with no anomalies. Cracking was observed in sample C3 prior to test. Several of the shocked plates showed similar cracking after heat treatment, and in many cases it was difficult to obtain sound specimens from the disks. At 1200°F (649°C) the data was primarily scattered around the mean.

23

TABLE 4. SHOCK WAVE PROCESSED TENSILE RESULTS

Plate No.	Yield Strength (ksi)	Yield Strength (MPa)	Ultimate Strength (ksi)	Ultimate Strength (MPa)	Elongation (%)	RA (%)	Temperature (°F)	Temperature (°C)
A1	190.7	1313.9	202.0	1391.8	3.5	4.0	1000	(538)
A3	175.1	1206.4	227.6	1568.2	16.0	14.2	1000	(538)
B2	172.3	1187.1	199.6	1375.2	6.5	5.5	1000	(538)
B3	163.4	1125.8	220.4	1518.6	27.5	28.4	1000	(538)
C2	178.9	1232.6	217.1	1495.8	9.0	8.2	1000	(538)
C2	175.2	1207.1	229.7	1582.6	21.0	24.6	1000	(538)
C3	168.9	1163.7	227.1	1564.7	21.5	22.3	1000	(538)
D1	176.3	1214.8	207.0	1426.2	8.5	8.2	1000	(538)
D3	168.0	1157.5	225.6	1554.4	21.0	19.9	1000	(538)
D3	169.5	1167.9	225.7	1555.1	20.0	19.6	1000	(538)
E2	183.4	1263.6	232.7	1603.3	18.0	20.4	1000	(538)
E3	167.5	1154.1	223.8	1542.0	19.0	17.4	1000	(538)
A2	182.0	1254.0	198.0	1364.2	14.5	16.0	1300	(704)
A3	174.7	1203.7	195.0	1343.6	17.5	16.0	1300	(704)
B1	173.4	1194.7	187.4	1291.2	17.5	22.9	1300	(704)
B3	160.9	1108.6	179.5	1236.8	26.0	29.7	1300	(704)
C1	184.4	1270.5	193.0	1329.8	12.5	14.1	1300	(704)
C3	169.0	1164.4	185.6	1278.8	16.5	19.2	1300	(704)
D2	177.1	1220.2	188.5	1298.8	16.0	19.9	1300	(704)
D3	169.1	1165.1	183.8	1266.4	17.5	17.5	1300	(704)
E1	162.8	1121.7	166.6	1147.9	3.5	2.4	1300	(704)
E1	177.6	1223.7	190.0	1309.1	17.5	21.0	1300	(704)
E3	171.1	1178.9	185.6	1278.8	19.0	18.2	1300	(704)

* Samples numbered 1 and 2 are shocked by the flyer plate process at 150 kbars. Samples numbered 3 are shocked by the direct contact method 2g/in.³.

TABLE 5. LCF TEST RESULTS IN-100

| Specimen No.	Δε (%)	Mean ε (%)	Cycles	Temperature (°F)	(°C)	CPM
A1	1.0	0.5	4,207	1000	(538)	5
A3	1.0	0.5	14,670	1000	(538)	5
A4	1.0	0.5	2,936	1000	(538)	5
B2	1.0	0.5	4,791	1000	(538)	5
B3	1.0	0.5	4,629	1000	(538)	5
B4	1.0	0.5	7,946	1000	(538)	5
B4	1.0	0.5	3,597	1000	(538)	5
C2	1.0	0.5	16,030	1000	(538)	5
C3	1.0	0.5	3,867	1000	(538)	5
C3	1.0	0.5	Defect	1000	(538)	5
C4	1.0	0.5	3,263	1000	(538)	5
D1	1.0	0.5	Defect	1000	(538)	5
D1	1.0	0.5	Defect	1000	(538)	5
D3	1.0	0.5	4,244	1000	(538)	5
D4	1.0	0.5	3,096	1000	(538)	5
E2	1.0	0.5	Failed Set Up	1000	(538)	5
E3	1.0	0.5	4,288	1000	(538)	5
E4	1.0	0.5	3,798	1000	(538)	5
PWA 1074 mean	1.0	0.5	4,550	1000	(538)	5
95% lower bound	1.0	0.5	910	1000	(538)	5
A2	1.0	0.5	1,911	1200	(649)	5
A2	1.0	0.5	425	1200	(649)	5
A3	1.0	0.5	3,165	1200	(649)	5
A4	1.0	0.5	2,870	1200	(649)	5
B1	1.0	0.5	3,745	1200	(649)	5
B3	1.0	0.5	2,456	1200	(649)	5
B3	1.0	0.5	1,708	1200	(649)	5
B4	1.0	0.5	Defect	1200	(649)	5
C1	1.0	0.5	245	1200	(649)	5
C3	1.0	0.5	Cracked Threads	1200	(649)	5
C4	1.0	0.5	1,861	1200	(649)	5
D2	1.0	0.5	1,859	1200	(649)	5
D3	1.0	0.5	1,517	1200	(649)	5
D4	1.0	0.5	2,129	1200	(649)	5
E1	1.0	0.5	4,858	1200	(649)	5
E3	1.0	0.5	5,381	1200	(649)	5
E4	1.0	0.5	1,574	1200	(649)	5
E4	1.0	0.5	Defects	1200	(649)	5
PWA 1074 mean	1.0	0.5	3,000	1200	(649)	5
95% lower bound	1.0	0.5	560	1200	(649)	5

*Samples No. 1 and 2 — shocked at 150 kbars (flyer plate)
Sample No. 3 — direct contact 2g/in.^{3}
Sample No. 4 — control (not shocked)
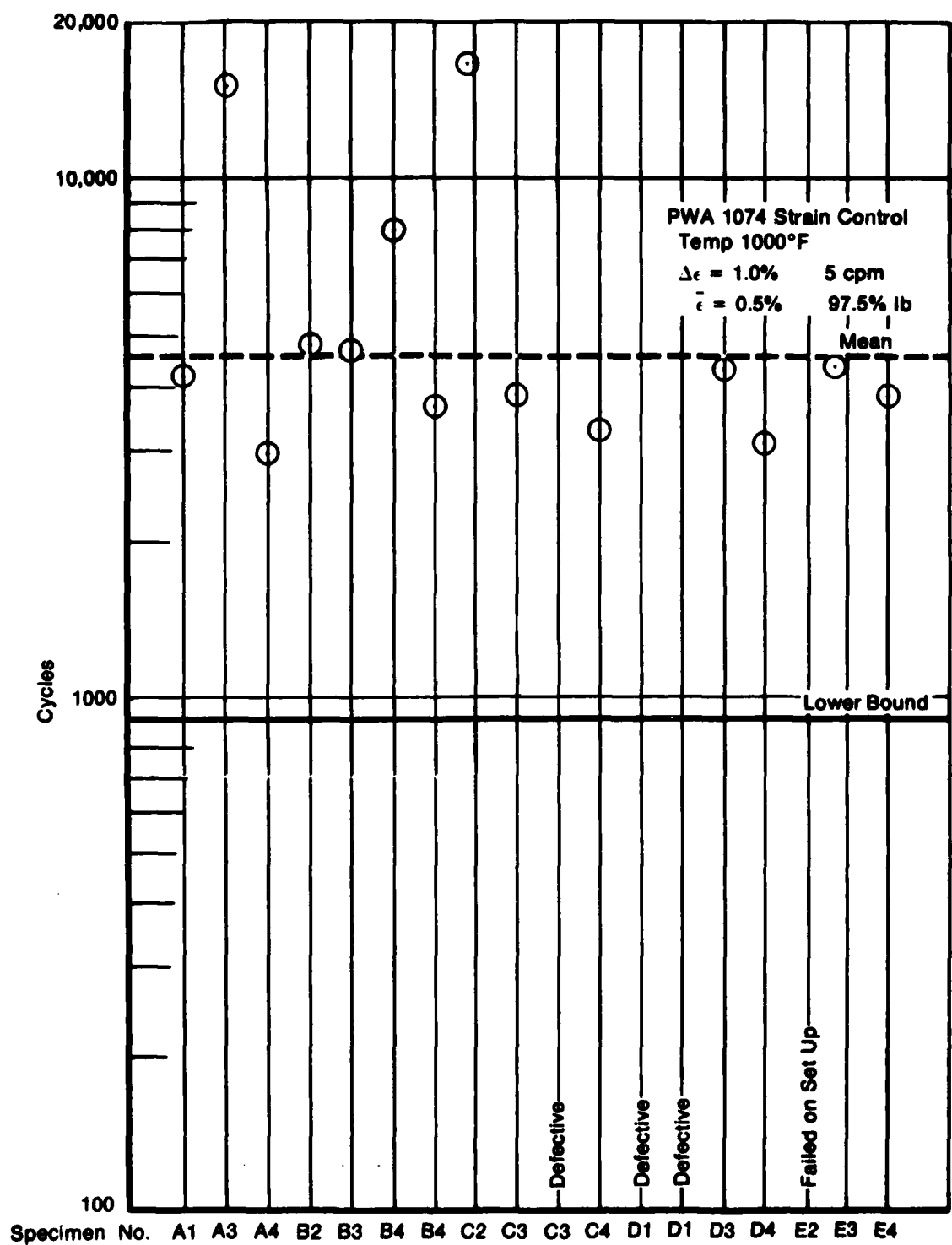
Figure 20.   Plot of LCF Results at 1000°F

26
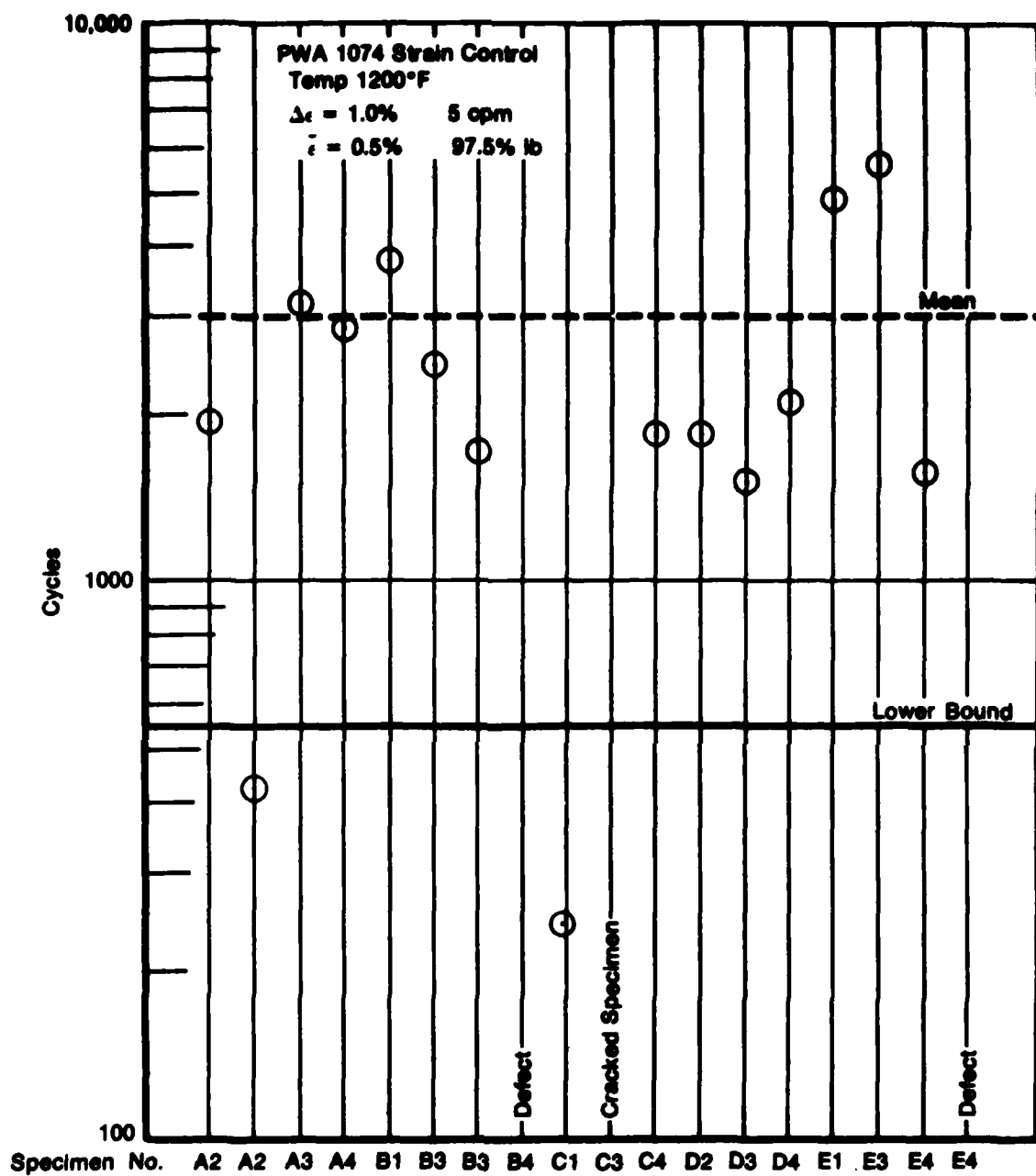
Figure 21.   Plot of LCF Results at 1200°F

27

Mag: 50X FAM 89611

Mag: 100X FAM 89613

Mag: 500X FAM 89615

FD 184259

Figure 22.   Fractographs of Low-Cycle Fatigue Specimen C2 Showing Internal Origin of Failure

28
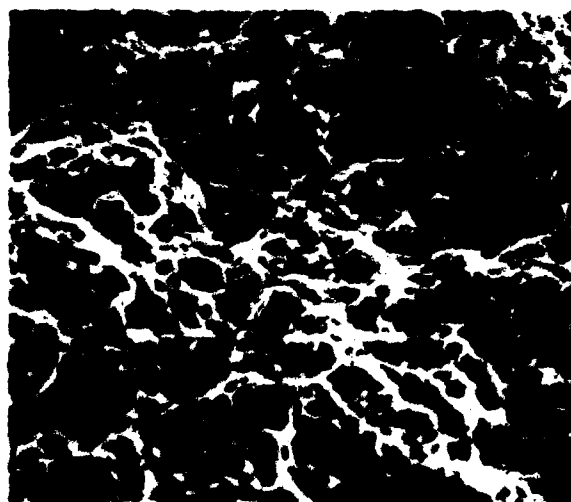
Mag: 20X   FAM 89986

Mag: 500X   FAM 89989

Mag: 2000X   FAM 89991

FD 184260

Figure 23   Fracture Surface of Low Cycle Fatigue Specimen E-2 Which Failed
             on Set-Up

29

METALLOGRAPHIC EVALUATION

Optical evaluation of specimens cut from shocked and fully heat treated samples was done on all heat treatments and processes. There was no observable variation in microstructure due to processing, as shown in Figure 24. The γ' morphology and size is essentially unchanged in the shocked and unshocked condition. This was the expected result since post shocking thermal treatments were below the temperature at which γ' coarsening takes place in IN-100. In addition, heat treatments C, D and E showed similar structures (Figure 25). The structure obtained from optical microscopy is primarily a function of the pre-shocking heat treatment, as shown in Figures 26 and 27, which show solution treated, standard aged, and overaged microstructures. It would be necessary to do transmission electron microscopy (TEM) to detect more subtle differences.

Etching of grain boundaries revealed a grain size of ASTM 12 that remained unchanged by either heat treatment or processing (Figures 28, 29 and 30).

Examination of thin foils prepared from heat treatments A, B and C was conducted to evaluate structure and dislocation structure. Figure 31 presents views of typical areas of samples A4, B4, and C4. Note the absence of dislocations in these samples. The few dislocations observed are located at twin boundaries and at γ-γ' interfaces (Figure 32). The difference in size of cooling γ' for the different heat treatments are depicted in Figure 33. While there was a pronounced absence of dislocations in the control samples, large numbers of dislocations were introduced in the shocked samples. Although absolute dislocation counts were not made, it appears that more dislocations were generated by the flyer plate method than by direct contact loading (Figure 34). This was expected due to higher strengths obtained by the flyer plate method. Dislocations were found at interfaces such as twin boundaries (Figure 35). There was also an anomaly that occurred during the TEM investigations. It appears that in sample B3, shocked by direct contact, there was a general alignment of dislocations parallel to one another (Figure 36). There is no explanation for this behavior at this time.

Mag: 1000X   Flyer Plate   FAM 89866   Mag: 1000X   Direct Contact   FAM 89870

Etch: Glyceregia   Etch: Glyceregia
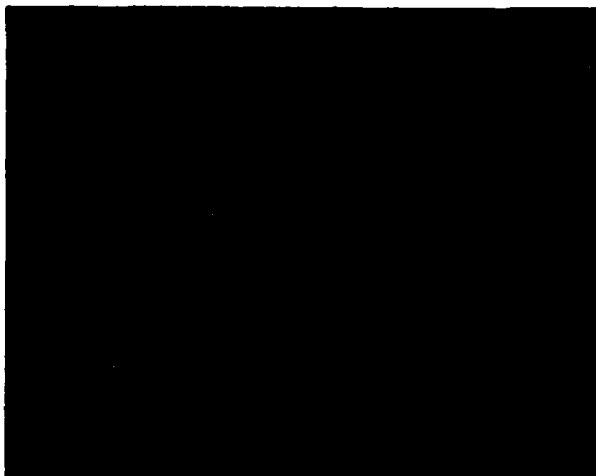
Mag: 1000X   Control   FAM 90333

Etch: Glyceregia

FD 184261

Figure 24. Heat Treatment "A" Showing No Effect on γ Due to Processing

31

Mag: 500X   FAM 90338   Mag: 500X   FAM 90336

Heat Treatment C   Heat Treatment D

Etch: Glyceregia   Etch: Glyceregia

Mag: 500X   FAM 90334

Heat Treatment E

Etch: Glyceregia

FD 184262

Figure 25.   Micrographs Showing Lack of Microstructural Variation With Heat Treatments C, D, and E
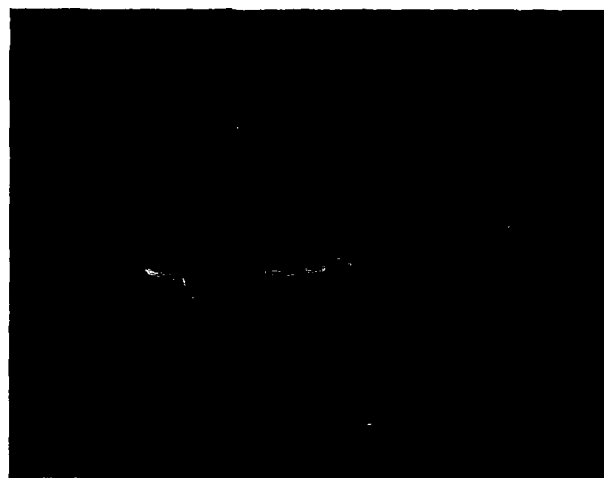
32

Mag: 500X   FAM 89865   Mag: 500X   FAM 89877

Heat Treatment A   Heat Treatment C

Etch: Glyceregia   Etch: Glyceregia

Mag: 500X   FAM 89871

Heat Treatment B

Etch: Glyceregia

FD 184263

Figure 26.   Variation in γ' Due to Various Preshock Aging Cycles With Heat Treatments A, C, and B

33

Mag: 1000X FAM 89866

Heat Treatment A

Etch: Glyceregia

Mag: 1000X FAM 89878

Heat Treatment C

Etch Glyceregia

Mag: 1000X FAM 89872
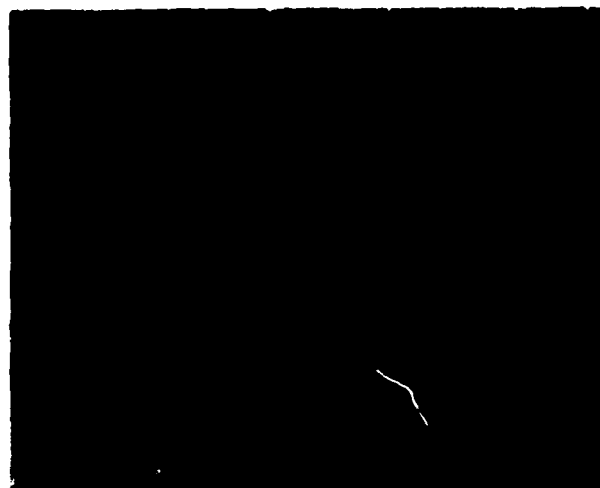
Heat Treatment B

Etch: Glyceregia

FD 184264

Figure 27. Variation in γ' Due to Various Preshock Aging Cycles With Heat Treatments A, C, and B

Mag: 500X   Heat Treatment A   FAM 90295   Mag: 500X   Heat Treatment B   FAM 90298

Etch: Kalling   Etch: Kalling

Mag: 500X   Heat Treatment C   FAM 90302

Etch: Kalling

FD 184265
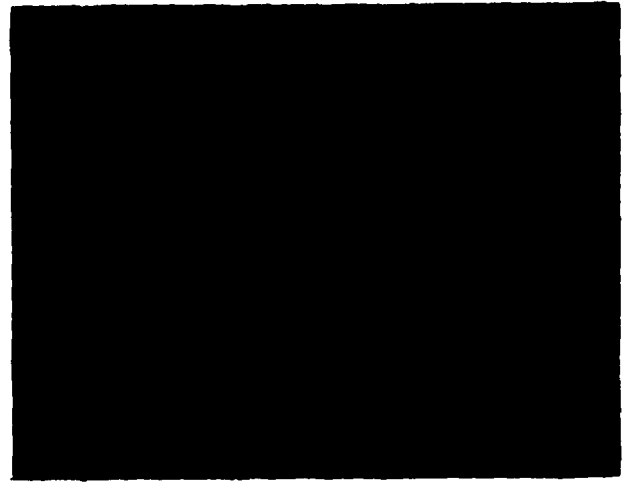
Figure 28. Lack of Grain Size Variation With Heat Treatments A, B, and C

35

Mag: 1000X   Heat Treatment A   FAM 90292   Mag: 1000X   Heat Treatment B   FAM 90299
Etch: Kalling   Etch: Kalling

Mag: 1000X   Heat Treatment C   FAM 90303
Etch: Kalling

FD 184266

Figure 29.   Lack of Grain Size Variation With Heat Treatments A, B, and C

36

Mag: 1000X   D1   FAM 90311   Mag: 1000X   D3   FAM 90310
Etch: Kallings   Etch: Kallings

Mag: 1000X   D4   FAM 90309
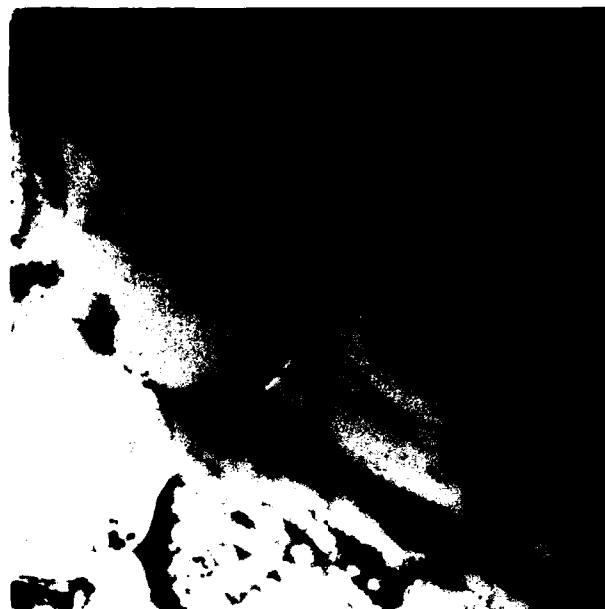Etch: Kallings

FD 184267

Figure 30.   *Effects of Processing on Grain Size Are Negligible. D1, Flyer Plate; D3, Direct Contact; D4, Control.*

37

Mag: 10,000X

A4

Mag: 10,000X
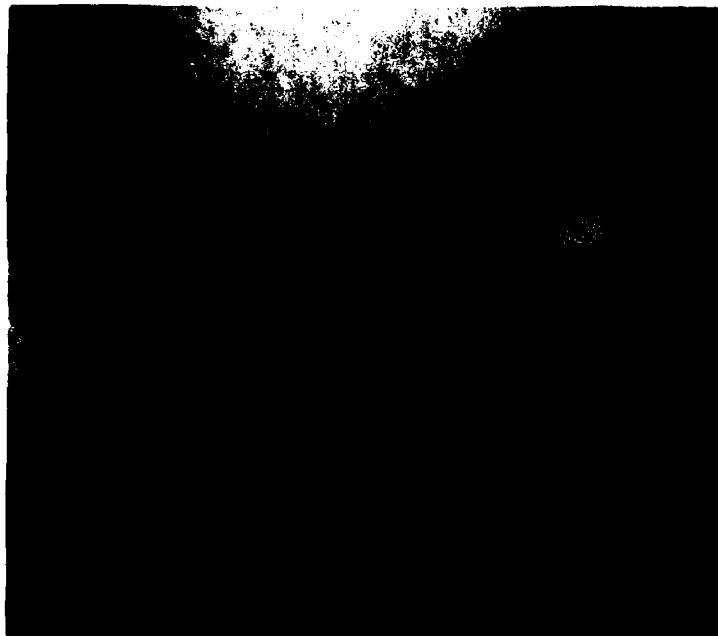
B4

Mag: 27,000X

C4

Mag: 36,000X

A4

FD 184268

Figure 31. General Areas of Thin Foils With Marked Absence of Dislocations

38

Mag: 98,000X

A4
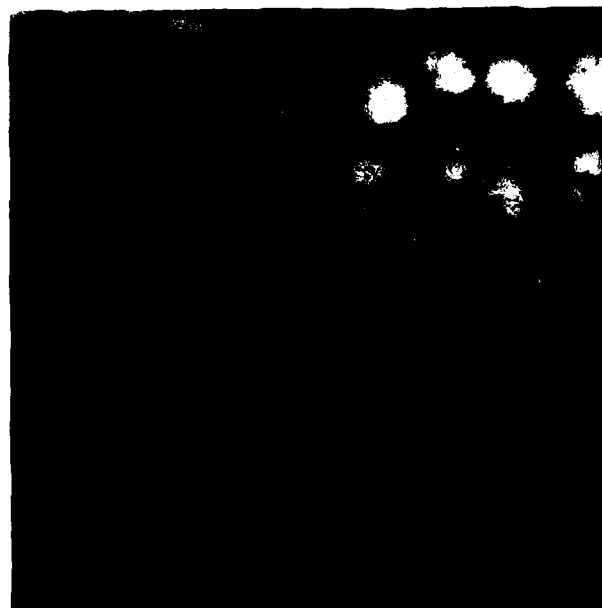
Mag: 98,000X

C4   FD 184269

*Figure 32.   Dislocations in the Control Samples Are Located at Twin Bound-
aries, A4, and γ γ' Interfaces, C4*

39

Mag: 27,000X

A4

Mag: 27,000X

B4

Mag: 27,000X

C4

FD 184270

Figure 33. Effects of Heat Treatments A, B and C on Size of Cooling γ
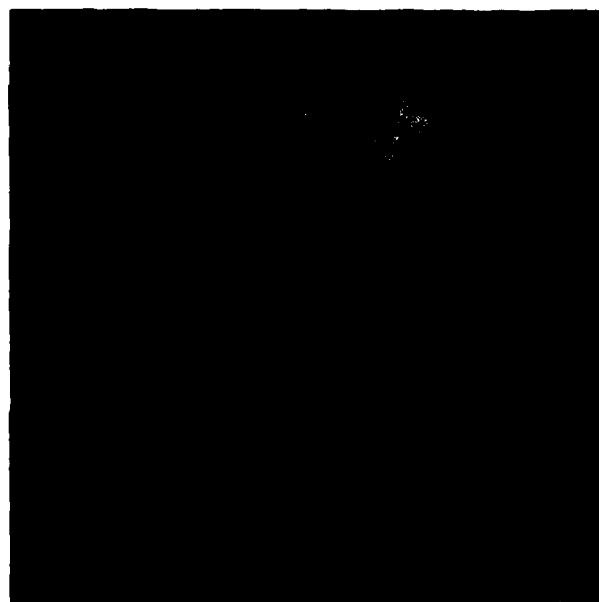
Mag: 36,000X

C1

Mag: 98,000X

C1

Mag: 36,000X

C3

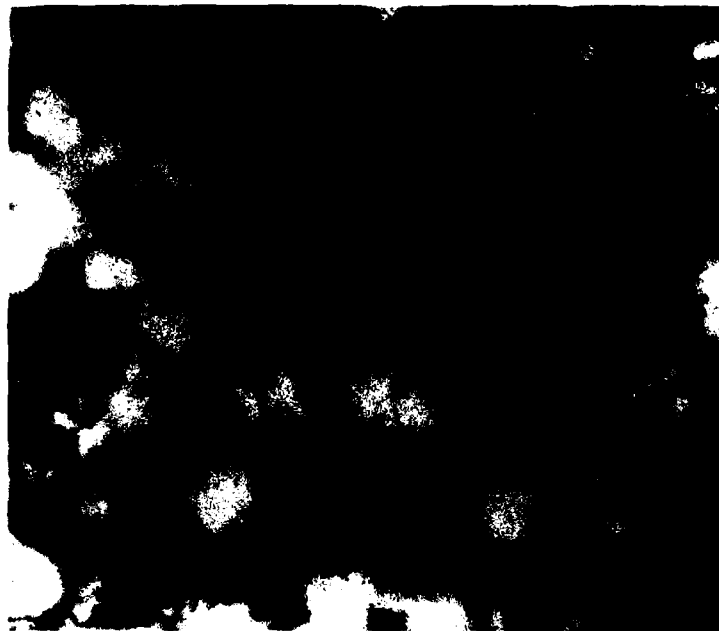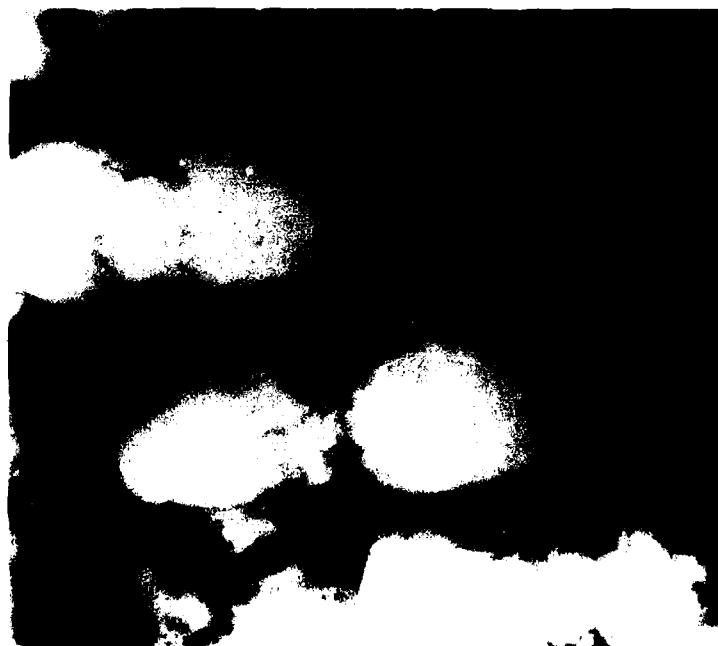Mag: 98,000X

C3

FD 184271

Figure 34.   The Density of Dislocations in γ' Is Affected by Processing Methods
C1, Flyer Plate; C3, Direct Contact

41

Mag: 47,000X

B1

Mag: 98,000X

B1

FD 184272

Figure 35. *Dislocations Located at Twin Boundary in Specimen Shocked Via the Flyer Plate Method*

42

Mag: 36,000X

B3

Mag: 98,000X

B3

FD 184273

*Figure 36. Anomalous Alignment of Dislocations in Sample Shocked by Direct
Contact Method*

43

SECTION V

CONCLUSIONS

On the basis of the experience gained in this program to date, it can be concluded that:

1. Shock wave thermomechanical processing of IN-100 disk materials offers enhancement of strength when compared to unshocked material, however ductility tends to decrease.

2. The flyer plate method of shocking offers higher strengths at 1300°F (704°C) than the direct contact method of shocking, but at lower ductilities.

3. There appeared to be no significant difference in the strength or LCF characteristics of IN-100 when varying the post-shocking heat treatment.

4. Results of LCF testing are inconclusive, however two samples of heat treatments C and A, (Standard heat treatment and Standard heat treatment without stress relief cycle) showed greater than 3X improvements in fatigue life at 1000°F (538°C).

5. Analysis of TEM work revealed that a dislocation substructure is in fact created by shock wave treatments, and it appears that the flyer plate method produces a higher density of dislocations than the direct contact method under the conditions studied.

SECTION VI

RECOMMENDATIONS

Heat treatments A and C conducted on IN-100 (MOD) appear the most promising from this program and further investigations into these thermal treatments should be undertaken. It seems necessary to increase the amount of testing done on such a program since it is very difficult to analyze data with only one or two points at each variable. In addition, since a dislocation substructure appears to be the strengthening mechanism, it would be beneficial to test creep or stress rupture in addition to tensile and LCF to determine if this substructure is substantially destroyed at disk service temperatures and over long periods of time. Finally additional study is required in shock processing methods themselves. The effects of other variables than pulse duration should be determined. In addition, multiple shocking at lower pressures should be considered to maintain disk integrity.

REFERENCES

1. Noland, M., H. Gadberry, J. Loser and E. Sneegas, "Explosive Metalworking," *High-Velocity Metalworking A Survey*, NASA Special Publication 5062, NASA Washington, 1967, pp 123-127.

2. University of Denver, Denver Research Institute, "Thermomechanical Processing of Nickel-Base Alloy AF2-1DA Using Shock Wave Deformation," Final Tech Report, Contract No. N62269-74-C-0281, to Naval Air Systems Command, June 1976.

3. University of Denver, Denver Research Institute, "Response of Nickel-Base Superalloys to Thermomechanical Processing by Shock Wave Deformation," Final Tech Report, Contract No. N62269-73-C-0376, to Naval Air Systems Command, April 1974.

4. University of Denver, Denver Research Institute, "Thermomechanical Processing of Nickel-Base Superalloys by Shock Wave Deformation, Final Tech Report, Contract No. N00019-72-0138, to Naval Air Systems Command, March 1973.

5. Mahajan, S., "Metallurgical Effects of Planar Shock Waves in Metals," Phy. Stat. Sol., Volume 2, 1970, p. 198.

6. Keh, A. S., *Direct Observations of Lattice Defect in Crystals*, Interscience Publishers, New York, 1962 p. 213.

7. Bailey, J. and P. B. Hirsch, Phil. Mag., Volume 5, 1960, p. 485.

8. Dieter, G., *Mechanical Metallurgy*, McGraw-Hill, Inc., 1961, p. 236.

9. Friedel, J., *Dislocations*, Pergamon Press, Oxford, 1964, p. 187.

10. Appleton, A. S. and J. S. Waddington, Phil. Mag., Volume 12, 1965, p. 273.

11. Peitteiger, L. A., "Explosive Hardening of Nickel Maraging and Manganese Steels," U.S. Naval Weapons Laboratory, Report No. 1934, September 1964.

12. Peitteiger, L. A., "Explosive Hardening of Iron and Low Carbon Steel," U.S. Naval Weapons Laboratory, Report No. 1950, October 1964.

13. Peitteiger, L. A., "The Effects of Explosively Induced Stress Waves on the Mechanical Properties of Seven Metals," U.S. Naval Weapons Laboratory, Report No. 1954, November 1964.

14. Orava, N. R., "Techniques for the Control and Application of Explosive Shock Waves," Dept. of Metallurgical Engineering — South Dakota School of Mines and Technology.

15. Otto, H. E., Proposal Revision to Pratt & Whitney Aircraft, University of Denver, Denver Research Institute, May 1977.

16. Mote, J. D., Technical Communications, University of Denver, Denver Research Institute.